Microscopic spectral density in random matrix models for chiral and diquark condensation

Benoît Vanderheyden

Departement of Electrical Engineering and Computer Science,

B-28, Université de Liège, Sart-Tilman,

B-4000 Liège, Belgium

A. D. Jackson

The Niels Bohr Institute, Blegdamsvej 17, DK-2100 Copenhagen Ø, Denmark

(Dated: August 12, 2009)

Abstract

We examine random matrix models of QCD which are capable of supporting both chiral and diquark condensation. A numerical study of the spectral densities near zero virtuality shows that the introduction of color in the interactions does not alter the one-body results imposed by chiral symmetry. A model with three colors has the spectral density predicted for the chiral ensemble with a Dyson index $\beta = 2$; a pseudoreal model with two colors exhibits the spectral density of the chiral ensemble with $\beta = 1$.

PACS numbers: 11.30. Fs, 11.30. Qc, 11.30. Rd, 12.38. Aw

Chiral random matrix theory (χRMT) is based on the observation that many of the low-energy properties of QCD are dominated by its global symmetries [1]. Random matrix models [2] thus attempt to capture the basic mechanisms for chiral condensation by reducing the QCD interactions to their essential structure. These models introduce low-lying modes which respect a basic left-right symmetry but which interact via random matrix elements. The consequences of chiral symmetry have been investigated at two levels. The microscopic level deals with the statistical properties of the eigenvalues of the Dirac operator and their correlations. Here, χRMT studies [3–5] have helped in understanding how these properties are determined by the spontaneous breaking of chiral symmetry as indicated, for example, by the universality of the spectral density near zero virtuality and associated sum rules [1]. At the macroscopic level, it is possible to consider the consequences of chiral symmetry for the global state of the random matrix system. With the aid of the mean field approximation and additional prescriptions for including the effects of temperature and chemical potential, it is straightforward to construct the partition function for χRMT models and thus examine the patterns of chiral symmetry breaking as a function of T, μ, and the quark mass [6, 7]. Many of the properties of the resulting phase diagram are direct consequences of chiral symmetry and largely independent of the detailed form of the interactions. They are thus expected to provide guidance in our understanding of the QCD phase diagram particularly in cases (e.g., $N_c = 3$ and $\mu \neq 0$) where the Dirac operator is non-Hermitean. These are cases where lattice simulations cannot rely on importance sampling and are very difficult to perform [8–11].

There has been considerable interest in the possibility that both chiral and diquark condensates can develop and compete thermodynamically in QCD. (For a review of diquark condensation in QCD, see [12–15].) Thus, we recently proposed a random matrix model for QCD which goes beyond χRMT and has interactions which implement coexisting chiral and color symmetries [16, 17]. We have examined this model at the macroscopic level by identifying the allowed topologies for the (T, μ) phase diagram. The phase structure is determined by a single parameter α, defined as a ratio between coupling constants in the chiral and diquark condensation channels. Physically, this ratio measures the relative strengths of the chiral and color symmetries in the random matrix interactions. In the cases relevant for QCD [either SU(2) or SU(3)], α has a fixed value and is associated with a given phase structure. The topology of this phase structure is robust with respect to moderate variations

in the detailed form of the interactions (i.e., variations in α).

The addition of color structure to the interactions implies additional constraints on the random matrix ensemble considered. As we shall see below, the color generators modify the statistical weights of the interaction matrix elements. The question then arises whether these constraints are capable of altering the various results associated with chiral symmetry alone. Our previous considerations suggest that this is not the case at the macroscopic level. In the case of an interaction which is completely dominated by chiral symmetry ($\alpha \to 0$), our models precisely reproduce the phase diagram of χRMT (Ref. [6]). In cases relevant for QCD with fundamental fermions [26] and three colors ($N_c = 3$ and $\alpha = 0.75$), the diquark phase develops in regions where it is thermodynamically advantageous, but color does not otherwise modify the phase structure. Thus, for $N_c = 3$, color does not seem to weaken the chiral correlations at the macroscopic level.

For $N_c = 2$, the situation is more subtle: the gauge interaction is pseudoreal, and baryons and mesons belong to the same multiplets. For $m = 0$, $\mu = 0$, and N_f flavors, the quark Lagrangian has an extended SU($2N_f$) invariance which relates chiral and diquark fields. This flavor symmetry is explicitly broken for either $m > 0$ or $\mu > 0$. Studies of the symmetry breaking patterns showed that a diquark condensed phase becomes favorable for $\mu \sim m_\pi \propto m^{1/2}$ and $T < T_c$ [18–21]. Our model exhibits the SU($2N_f$) symmetry and produces results which agree with the general predictions of Ref. [18] as well as with those of chiral perturbation theory [19, 21]. Thus, for $N_c = 2$, the introduction of color in the random matrix interactions does not lead to unexpected topologies of the phase diagram (i.e. unexpected macroscopic properties).

The purpose of this paper is to investigate the consequences of the additional color correlations at the microscopic level. To this end, we examine the distributions of the eigenvalues of the Dirac operator near zero virtuality and compare them with the analytic forms predicted by χRMT. The rest of the paper is organized as follows: We present the models in Sec. I, discuss aspects of their macroscopic and microscopic spectral densities in Secs. II and III, comment on other properties in Sec. IV, and conclude in Sec. V.

I. THE RANDOM MATRIX MODELS

To understand the form of the correlations induced by each symmetry, it is useful to provide a brief description of the models of Refs. [16], which we will refer to as I. In the present paper we will restrict our attention to a theory with N_f light flavors, zero temperature, zero chemical potential, and zero quark mass. We start by recalling the basic form of chiral random matrix theory, in which only chirality is introduced, and then extend the model to include color.

We consider first a chiral random matrix model and work in the sector of zero topological charge for simplicity. The partition function has the form

$$Z = \int DW \prod_{i=1}^{N_f} D\psi_i^* \, D\psi_i \, \exp\left[i \sum_{i=1}^{N_f} \psi_i^* \, \mathcal{D} \, \psi_i \right] \exp\Big(- \frac{N\beta\Sigma^2}{2} \mathrm{Tr}[WW^\dagger] \Big), \tag{1}$$

where ψ_i and ψ_i^* are independent Grassmann variables representing the quark fields and where the matrix $\mathcal{D}$ represents the Dirac operator. Its block structure reflects chiral symmetry. Working in a suitable basis of left and right states $(1 \pm \gamma_5)\phi_n$, $\mathcal{D}$ has the form [2]

$$\mathcal{D} \, = \, \begin{pmatrix} 0 & W \\ W^\dagger & 0 \end{pmatrix}, \tag{2}$$

where W is an $N \times N$ block matrix. The integral in Eq. (1) is over the matrix elements of W, DW is a Haar measure, and Tr denotes a trace over the N matrix indices. The model is thus a theory of $2N$ low-lying modes which respect chiral symmetry and whose interaction matrix elements W_{ij} are drawn on a Gaussian distribution. The number of modes scales with the volume of the system; the thermodynamic limit is taken as $N \to \infty$.

For later comparisons, it is useful to understand how the gauge group is taken into account. In a model which implements the global symmetries of QCD with $N_c = 3$, the matrix elements of W are complex. For the analysis below, it is worth noting that their real and imaginary parts satisfy no particular relationship and are thus drawn independently. This case corresponds to a Dyson index $\beta = 2$ and is described by the chiral unitary ensemble (χGUE). For $N_c = 2$, the gauge group is pseudoreal as mentioned above. The Dirac operator then contains an additional antiunitary symmetry [2], which allows one to choose a basis in which the matrix elements of W are real. This case leads to the chiral orthogonal ensemble (χGOE). In short, the value of N_c enters χRMT only through the reality of the matrix elements of W.

In model I, we included color directly in the interactions in a way which mimics single-gluon exchange. For two flavors, the partition function takes the form

$$Z = \int DH \; D\psi_1^\dagger \, D\psi_1 \, D\psi_2^* \, D\psi_2^T \, \exp\left[i \begin{pmatrix} \psi_1^\dagger \\ \psi_2^T \end{pmatrix}^T \begin{pmatrix} \mathcal{D}_c & 0 \\ 0 & -\mathcal{D}_c^T \end{pmatrix} \begin{pmatrix} \psi_1 \\ \psi_2^* \end{pmatrix} \right], \tag{3}$$

where ψ_1 and ψ_2^T denote the quark fields for flavor 1 and flavor 2, respectively, DH is a measure to be defined below, and $\mathcal{D}_c$ is the single-quark Dirac operator. Note that the subblock associated with flavor 2 has been transposed in order to exhibit the possibility of forming $\langle \psi_2^T \psi_1 \rangle$ condensates (see I).

The diagonal block $\mathcal{D}_c$ now reflects both chiral and color symmetries. In order to be able to define an order parameter which is antisymmetric under the permutation of an odd number of quantum numbers, spin has to be introduced together with color [16]. The Dirac operator $\mathcal{D}_c$ then has the chiral structure of Eq. (2) where W is exploded into a $2N_c \times 2N_c$ matrix of embedded spin and color subblocks,

$$W = \sum_{\mu=0}^{3} \sum_{a=1}^{N_c^2-1} (\sigma_\mu \otimes \lambda_a) \, A_{\mu a}. \tag{4}$$

Here $\sigma_\mu = (1, i\vec{\sigma})$ are 2×2 spin matrices, λ_a are the $N_c \times N_c$ matrices of SU(N_c) and $A_{\mu a}$ are $n \times n$ real matrices representing the gluon fields. Taking into account all substructures, each matrix W is thus $N \times N$ with $N = 2N_c n$. The matrix elements of $A_{\mu a}$ in Eq. (4) are distributed according to the measure DH, Eq. (3), which takes the form

$$DH = \left\{ \prod_{\mu a} DA_{\mu a} \right\} \exp\left(-N\Sigma_0^2 \sum_{\mu a} \mathrm{Tr}[A_{\mu a} \, (A_{\mu a})^T] \right), \tag{5}$$

where $DA_{\mu a}$ are Haar measures, Σ_0 is a constant, and the superscript T denotes a transposition. Again, the thermodynamic limit corresponds to $N \to \infty$.

Evidently, these spin and color substructures impose strong constraints between the real and imaginary parts of the matrix elements of W. Consider, for example, the contributions to $\mathcal{D}_c$, Eqs. (3) and (4), of the random matrices A_{01} ($\mu = 0$ and $a = 1$) and A_{02}. Their matrix elements are real and are drawn independently. When combined to form W as prescribed in Eq. (4), the matrix elements of A_{01} multiply σ_0, a real diagonal spin matrix, and λ_1, a real color matrix. Hence, A_{01} contributes to the real part of W only. Similarly, the matrix elements of A_{02} combine with σ_0 (real) and λ_2, an imaginary color matrix. They thus contribute to the imaginary part of W. Hence, in contrast to ordinary χRMT, the matrix

elements of W are complex for both $N_c = 3$ and $N_c = 2$. The real and imaginary parts of W arise from well-defined combinations of the matrix elements of $A_{\mu a}$. Their statistical distributions are then dictated by the content of the spin and color block matrices, which thus introduce well-defined correlations.

Do these additional correlations preserve those imposed in Eq. (2) by chiral symmetry? The W matrix elements are complex for all N_c; their real and imaginary parts are no longer independent random variables. One might thus be concerned that the statistical properties of the eigenvalues of the Dirac operator would differ from those of the χGUE and χGOE. We now consider a number of spectral properties to indicate that this is *not* the case and that the additional color symmetries do not alter the statistical properties due to chiral symmetry.

II. THE MACROSCOPIC SPECTRAL DENSITY

As an initial measure of the statistical properties, we consider the spectral density $\rho(\lambda)$, defined as

$$\rho(\lambda) \equiv \frac{1}{2N} \left\langle \sum_{i=1}^{2N} \delta(\lambda - \lambda_i) \right\rangle, \tag{6}$$

where λ_i are the $2N$ eigenvalues of the Dirac operator and $\langle\rangle$ denotes an ensemble average. While $\rho(\lambda)$ is not universal in the usual random matrix sense, we will focus on those symmetry properties which are expected to be protected. Consider first the chiral random matrix model defined in Eq. (1). Because of the block structure of $\mathcal{D}$, Eq. (2), the eigenvalues λ_i occur in pairs of opposite signs. Moreover, Eq. (1) shows that the spectrum is N_f-fold degenerate. Consider next model I, Eq. (3), which may seem different at first glance because of its more elaborate structure. In fact, each flavor subblock has the same chiral substructure as in Eq. (2), and the eigenvalue spectrum remains symmetric about $\lambda = 0$. Further, the eigenvalues of $-\mathcal{D}_c^T$, Eq. (3), are degenerate with those of $\mathcal{D}_c$ so that the spectrum is again twofold degenerate ($N_f = 2$). Hence, the same basic chiral and flavor symmetries prevail in the two models.

In order to facilitate numerical evaluation, we now consider the quenched limit $N_f \to 0$. This limit is free from contributions from vacuum graphs (through powers of the determinant of the Dirac operator in the partition function; see [1]). The ensemble average of a

given quantity then amounts to a mere counting of the contributions from the individual eigenvalues of $\mathcal{D}$ (or $\mathcal{D}_c$), distributed according to the normal laws of Eq. (1) or Eq. (5), as appropriate.

For large matrices, we find that the model I is numerically consistent with the (non universal) semicircle law familiar from the χGUE and χGOE,

$$\lim_{N\to\infty} \rho(\lambda) \;=\; \begin{cases} \frac{\Sigma}{\pi}\sqrt{1-\left(\frac{\Sigma\lambda}{2}\right)^2} & \text{if } |\lambda| \le 2/\Sigma, \\ 0 & \text{otherwise.} \end{cases} \tag{7}$$

In the case of chiral random matrix models, Σ is the variance of the distribution in Eq. (1). In model I, Σ is proportional to Σ_0, Eq. (5), in a manner that will be discussed shortly. Note that thanks to the Banks-Casher relationship [22], Σ is in all cases to be identified with the chiral order parameter:

$$\langle\bar{\psi}\psi\rangle = \lim_{\lambda\to 0}\lim_{N\to\infty} \pi\rho(\lambda) = \Sigma. \tag{8}$$

Having obtained the semicircle distribution in model I is a natural result. The random matrix interactions of Eq. (4) mix a set of $4\times(N_c^2-1)$ independent real matrices, $A_{\mu a}$, in a democratic way. This ensemble naturally leads to the semicircle law familiar from most elementary random ensembles, including the chiral ones.

Further remarks can be made about the dependence of Σ with respect to N_c. For χRMT, Σ does not depend on β, and hence does not depend on N_c. In model I, however, Σ is a function of N_c and Σ_0 which can be easily determined by noting the following relationship [27] between the radius of the semicircle $2/\Sigma$ and the variance $\langle \mathrm{Tr}[WW^\dagger]\rangle$:

$$\langle \mathrm{Tr}[WW^\dagger]\rangle = \frac{N}{\Sigma^2}. \tag{9}$$

From the definition of W, Eq. (4), and the distribution in Eq. (5), we have

$$\langle \mathrm{Tr}[WW^\dagger]\rangle = 4\sum_{\mu a}\langle \mathrm{Tr}[A_{\mu a}(A_{\mu a})^T]\rangle = \frac{2(N_c^2-1)}{N_c^2}\,\frac{N}{\Sigma_0^2}, \tag{10}$$

which gives

$$\Sigma \;=\; \frac{N_c}{\sqrt{2\,(N_c^2-1)}}\;\Sigma_0 = \begin{cases} 0.75\,\Sigma_0 & \text{if } N_c = 3, \\ \\ 0.8165\,\Sigma_0 & \text{if } N_c = 2. \end{cases} \tag{11}$$

The N_c dependence of the chiral condensate reflects the fact that the strength of the interactions in the chiral channel varies with N_c. In fact, the N_c-dependent prefactor in Eq. (10) is directly proportional to the Fierz coefficient which appears when the random matrix interactions are projected onto the chiral condensation channel (Ref. [16]).

III. THE MICROSCOPIC SPECTRAL DENSITY

The structures that are characteristic of chiral symmetry are most clearly seen in the distributions of the eigenvalues near zero virtuality. It is thus worth considering the microscopic spectral density, defined at the level of single eigenvalues as

$$\rho_S(z) = \lim_{N\to\infty} \frac{1}{2N\Sigma}\,\rho\left(\frac{z}{2N\Sigma}\right), \tag{12}$$

where Σ is the chiral order parameter of the theory at hand. The microscopic spectral densities of the various chiral ensembles are strikingly different. In the quenched limit, χGUE gives

$$\rho_S(z) \;=\; \frac{z}{2}\,\Big(J_0^2(z) + J_1^2(z)\Big) \qquad (\chi\text{GUE}, N_f = 0, z > 0), \tag{13}$$

while χGOE gives [1, 23, 24]

$$\rho_S(z) \;=\; \frac{z}{2}\,\Big(J_1^2(z) - J_0(z)\,J_2(z)\Big) - \frac{1}{2}\,J_0(z)\,\left(\int_0^z du\; J_2(u) - 1\right)$$
$$(\chi\text{GOE}, N_f = 0, z > 0). \tag{14}$$

Figures 1 and 2 show the histograms obtained in the models of Refs. [16], plotted against Eq. (13) for the model with $N_c = 3$ and against Eq. (14) for that with $N_c = 2$. The data were obtained from an ensemble of 2×10^5 matrices with blocks W of size 120×120 (i.e., $2nN_c = 120$). As in χRMT, the behavior of the small eigenvalues depends strongly on whether $N_c = 3$ or $N_c = 2$. In fact, the data agree with the theoretical curves for the corresponding chiral ensembles to expected statistical accuracy. The microscopic spectral density thus appears to preserve the form dictated by chiral symmetry in spite of the presence of additional color symmetries. In particular, we observe the familiar depletion near $z = 0$ for $N_c = 3$.

The spectrum in Fig. 2 is flatter than that for $N_c = 3$. This is a consequence of the greater motion of the individual eigenvalues in the model with $N_c = 2$. This difference is

familiar in chiral ensembles, where it is interpreted as a consequence of the fact that the spectrum of a real matrix (χGOE) is less rigid than that of a complex matrix (χGUE). It is interesting to see that the level motion in our model with $N_c = 2$ agrees with that expected for χGOE even though the matrix elements of W are no longer real. Again, the correlations induced by chiral symmetry are maintained in spite of the additional constraints introduced by the color structure of W.

Of course, the preservation of the $N_c = 2$ microscopic spectral density in spite of the complexity of W should not come as a surprise. The interactions in Eq. (3) are, in fact, pseudoreal when $N_c = 2$ [17]. Thus, we could have used an appropriate basis of states such that all matrix elements have vanishing imaginary parts. The model would then have displayed a greater similarity to a χRMT model with $\beta = 1$, and it would thus be natural to find a spectrum which reproduces that of χGOE.

IV. OTHER SPECTRAL PROPERTIES

We have also studied short range eigenvalue correlations by examining the distribution of level spacings, $p(s)$. Here, s is the nearest neighbor spacing measured in units of the local average spacing. (Hence, the average value of s is 1 by definition.) Note that $p(s)$ is a bulk observable which is sensitive to chiral symmetry only for small s. Figure 3 shows the relative difference between the results obtained for the model of I with $N_c = 3$ and those of the χGUE. The data were obtained from a set of nine independent series of diagonalizations of 10000 matrices of size $N \times N = 120 \times 120$. To avoid side effects due to the finite range of the random matrix support, we only kept a central portion of the spectrum (30th eigenvalue to 90th). The level spacing distribution for a given model is taken as a bin-by-bin average over the nine series of runs, with error bars corresponding to the variance in each bin. The plot shows $\delta p(s) = [p_{\chi\mathrm{GUE}}(s) - p_{N_c=3}(s)]/p_{\chi\mathrm{GUE}}(s)$, where $p_{\chi\mathrm{GUE}}(s)$ is the level spacing distribution for χGUE and $p_{N_c=3}(s)$ is that for model I with $N_c = 3$. [Note that $p_{\chi\mathrm{GUE}}(s) = p_{\mathrm{GUE}}(s)$.] The level spacing difference is everywhere consistent with zero. Similar results were obtained for a comparison with χGOE. Thus, the level spacing distribution reveals no statistically significant differences between the models of Refs. [16] and their corresponding chiral ensembles.

It is also useful to construct the variance-covariance matrix D, defined as

$$D_{ij} = \langle (\lambda_i - \bar{\lambda}_i)(\lambda_j - \bar{\lambda}_j) \rangle, \tag{15}$$

where $\bar{\lambda}_i$ is the mean value of eigenvalue i. Numerical studies of the models of Refs. [16] indicate that all eigenvalues of D are greater than zero. Thus, the eigenvalues of the Dirac operator do not satisfy any linear constraints. The eigenvalues of D are related to the statistically independent fluctuations of the eigenvalues of the Dirac operator about their mean values. (This relation would be exact if the joint probability distribution for the eigenvalues of the Dirac operator were strictly Gaussian.) Numerical studies reveal good agreement with the spectrum of normal modes known analytically for the χGOE and χGUE [25]. This provides an additional indication that the inclusion of color symmetry has not altered the statistical properties of the models of Refs. [16] from those of the corresponding chiral ensembles.

V. CONCLUSIONS

We have investigated a number of properties of the eigenvalue spectrum of random matrix models which include both chiral and color symmetries. We find no deviation from the analytic results of χRMT for either the microscopic spectral density or the level spacing distribution. Given the relatively elaborate block structure of these models, such studies are most easily performed numerically. While more complicated spectral correlators have not been investigated, we find no grounds to doubt that they will also reflect the underlying chiral structure of the problem. (It should be emphasized that this extended block structure does not lead to complicated forms for the partition function and that studies of the macroscopic properties of these models are straightforward for all T and μ.) The spin and color block structures of the interactions do not seem to upset spectral features associated with chiral symmetry. Rather, these additional correlations appear to act in a channel which is "orthogonal" to the chiral channel. We do not regard this result as surprising. One may think of the models of Refs. [16] as schematic lattice calculations which implement single-gluon exchange between discrete quark fields. This "lattice calculation" does not possess any other length scale than that introduced by Σ and is, hence, free of a Thouless energy. Because chiral symmetry is respected by the interactions, the results of χRMT should be

anticipated at all small energies. This is indeed what our numerical analysis reveals.

The inclusion of color does, of course, introduce additional correlations in the spectrum of the Dirac operator. It would be of interest to construct new spectral measures which could probe these correlations. In particular, it would be valuable to find a color analogue of the Banks-Casher relation to facilitate the determination of the strength of the diquark condensate.

Acknowledgments

We thank J. J. M. Verbaarschot for provocative questions which initiated this work and D. Toublan and K. Splittorff for useful discussions.

---

[1] For a review of χRMT, see J. J. M. Verbaarschot and T. Wettig, Annu. Rev. Nucl. Part. Sci. **50**, 343 (2000).

[2] E. V. Shuryak and J. J. M. Verbaarschot, Nucl. Phys. **A560**, 306 (1993); J. J. M. Verbaarschot, Phys. Rev. Lett. **72**, 2531 (1994); Phys. Lett. B **329**, 351 (1994).

[3] J. J. M. Verbaarschot and I. Zahed, Phys. Rev. Lett. **70**, 3852 (1993).

[4] J. J. M. Verbaarschot, Nucl. Phys. **B427**, 534 (1994).

[5] J. J. M. Verbaarschot, Nucl. Phys. **B426[FS]**, 559 (1994).

[6] A. D. Jackson and J. J. M. Verbaarschot, Phys. Rev. D **53**, 7223 (1996).

[7] M. A. Halasz, A. D. Jackson, R. E. Schrock, M. A. Stephanov, and J. J. M. Verbaarschot, Phys. Rev. D **58**, 096007 (1998).

[8] M. G. Alford, A. Kapustin, and F. Wilczek, Phys. Rev. D **59**, 054502 (1999).

[9] S. Chandrasekharan and U. J. Wiese, Phys. Rev. Lett. **83**, 3116 (1999).

[10] Z. Fodor and S. D. Katz, Phys. Lett. B **534**, 87 (2002); J. High Energy Phys. **03**, 014 (2002).

[11] P. de Forcrand and O. Philipsen, Nucl. Phys. **B642**, 290 (2002).

[12] B. Barrois, Nucl. Phys. **B129**, 390 (1977); D. Bailin and A. Love, Phys. Rep. **107**, 325 (1984).

[13] R. Rapp, T. Schäfer, E. V. Shuryak, and M. Velkovsky, Phys. Rev. Lett. **81**, 53 (1998); Ann. Phys. (N.Y.) **280**, 35 (2000).

[14] M. Alford, K. Rajagopal, and F. Wilczek, Phys. Lett. B **422**, 247 (1998).

[15] For a review on color superconductivity, see K. Rajagopal and F. Wilczek, *B. L. Ioffe Festschrift, At the frontier of particle physics/Handbook of QCD*, edited by M. Shifman (World Scientific, 2001), Vol. 3, p. 2061 hep-ph/0011333.

[16] B. Vanderheyden and A. D. Jackson, Phys. Rev. D **61**, 076004 (2000); **62**, 094010 (2000).

[17] B. Vanderheyden and A. D. Jackson, Phys. Rev. D**64**, 074016 (2001).

[18] J. B. Kogut, M. A. Stephanov, and D. Toublan, Phys. Lett. B **464**, 183 (1999).

[19] J. B. Kogut, M. A. Stephanov, D. Toublan, J. J. M. Verbaarschot, and A. Zhitnitsky, Nucl. Phys. **B582**, 477 (2000).

[20] K. Splittorff, D. T. Son, and M. A. Stephanov, Phys. Rev. D **64**, 016003 (2001).

[21] K. Splittorff, D. Toublan, and J. J. M. Verbaarschot, Nucl. Phys. **B620**, 290 (2002).

[22] T. Banks and A. Casher, Nucl. Phys. **B169**, 103 (1980).

[23] P. J. Forrester, P. Nagao, and G. Honner, Nucl. Phys. **B533**, 601 (1999).

[24] B. Klein and J. J. M. Verbaarschot, Nucl. Phys. **B588**, 483 (2000).

[25] A. D. Jackson, C. B. Lang, M. Oswald, and K. Splittorff, Nucl. Phys. **B616**, 233 (2001).

[26] In this work, we consider only fundamental fermions. For models with adjoint fermions, see [1, 19–21]

[27] This can be established by considering the resolvent operator $G(z) = \langle \mathrm{Tr}(z - D)^{-1} \rangle$, and by matching its asymptotic expansion at large z to the form it assumes for the spectral density of Eq. (7).

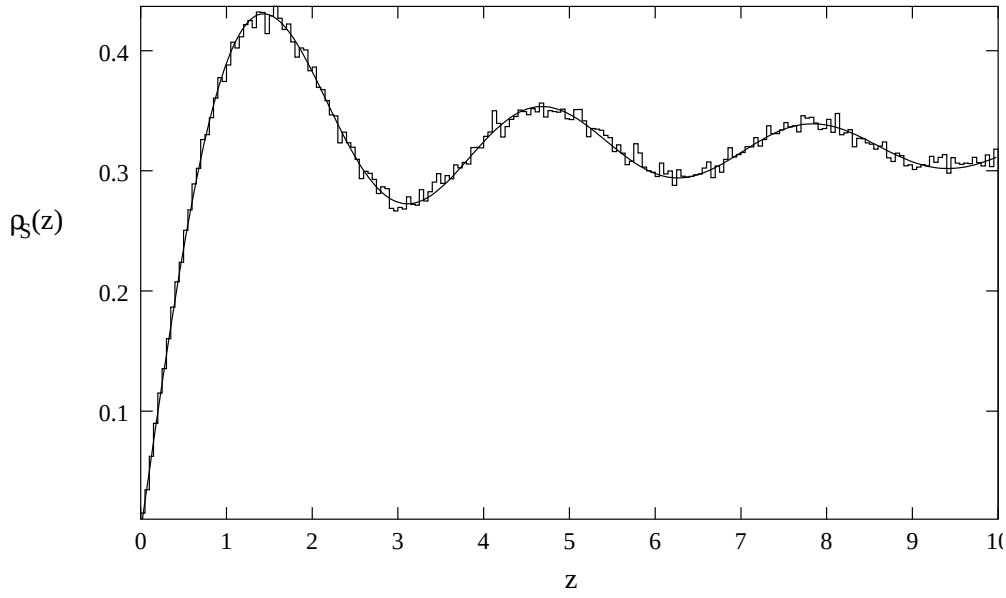

FIG. 1: Histogram: microscopic spectral density of the Dirac operator for a random matrix model with a color subblock and $N_c = 3$. Solid line: spectral density predicted for χGUE ($N_f \to 0$).

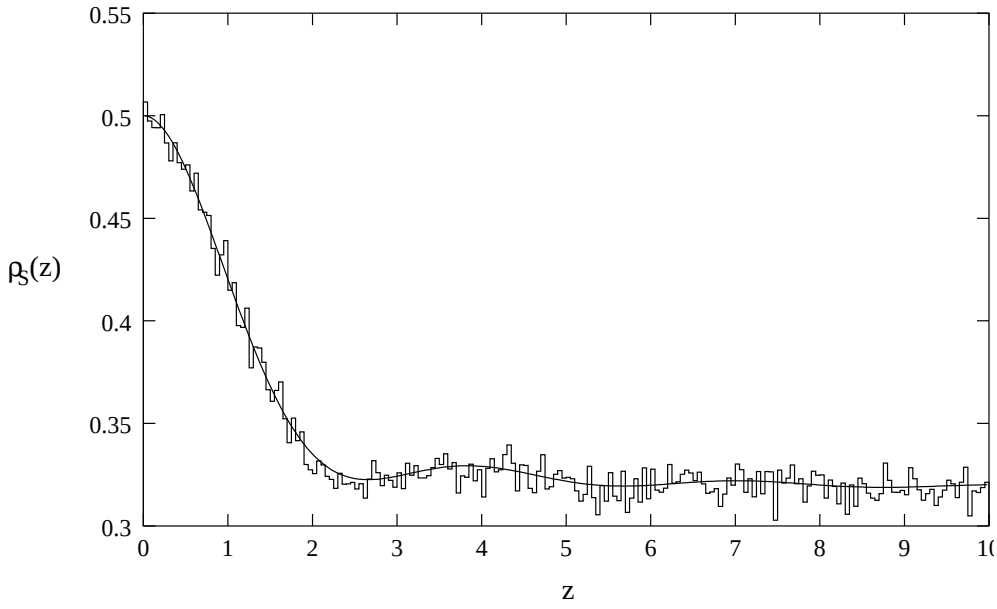

FIG. 2: Histogram: microscopic spectral density of the Dirac operator for a random matrix model with a color subblock and $N_c = 2$. Solid line: spectral density predicted for χGOE ($N_f \to 0$).

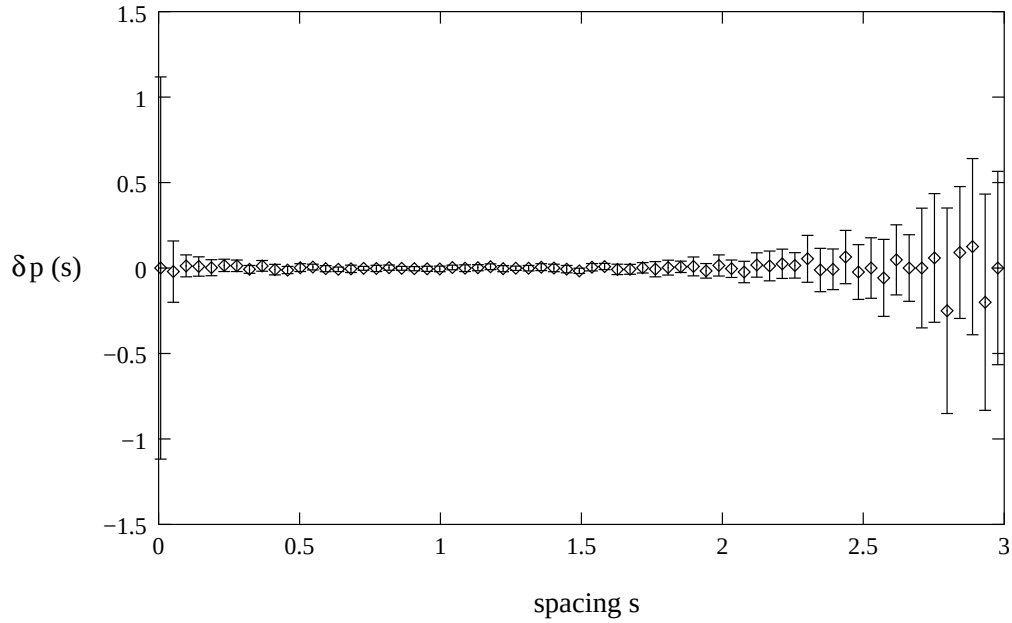

FIG. 3: Relative difference between the mean level spacing distribution for χGUE and that for a model with a color subblock and $N_c = 3$. The errorbars are estimated from a series of nine independent runs of diagonalizations.